

# Non-cyanobacterial diazotrophs dominate dinitrogen fixation in biological soil crusts at the early stage of crust formation.

Charles Pepe-Ranney<sup>1</sup>, Chantal Koechli<sup>1</sup>, Ruth Potrafka<sup>2</sup>, Ferran Garcia-Pichel<sup>2</sup>, Daniel H Buckley<sup>1,\*</sup>

<sup>1</sup>Cornell University, Department of Crop and Soil Sciences, Ithaca, NY, USA

<sup>2</sup>Arizona State University, School of Life Sciences, Tempe, AZ 85287, USA.

Correspondence\*:

Daniel H Buckley

Cornell University, Department of Crop and Soil Sciences, Ithaca, NY, USA,

## 1 ABSTRACT

Biological soil crusts (BSC) cover a vast global area and are key components of ecosystem productivity in arid soils. In particular, BSC contribute significantly to the nitrogen (N) budget in arid ecosystems via N<sub>2</sub>-fixation. N<sub>2</sub>-fixation in mature crusts is largely attributed to heterocystous cyanobacteria, however, early successional crusts are dominated by non-heterocystous cyanobacteria and this suggests that microorganisms other than cyanobacteria mediate N<sub>2</sub>-fixation during the early stages of BSC development. DNA stable isotope probing (DNA-SIP) with <sup>15</sup>N<sub>2</sub> revealed that *Clostridiaceae* and *Proteobacteria* are the most common microorganisms to assimilate <sup>15</sup>N in early successional 'light' crusts. The maximum relative abundance of <sup>15</sup>N<sub>2</sub>-assimilating taxa in the BSC was 0.00225% and 0.00127% for taxa that belong to *Clostridiaceae* and *Proteobacteria*, respectively. Their low abundance may explain why these heterotrophic diazotrophs have not previously been characterized in BSC. Diazotrophs play a critical role in BSC formation and characterization of these organisms represents a crucial step towards understanding how anthropogenic change will effect the formation and ecological function of BSC in arid ecosystems.

## 2 INTRODUCTION

Biological soil crusts (BSC) are specialized microbial mat communities that form at the soil surface in arid environments and fill a variety of important ecological functions in arid ecosystems. BSC occupy plant interspaces and cover a wide, global geographic range (Garcia-Pichel et al., 2003b). The ground cover of BSC on the Colorado Plateau has been measured as high as 80% by remote sensing (Karnieli et al., 2003). The global biomass of BSC *Cyanobacteria* alone is estimated at 54 x 10<sup>12</sup> g C (Garcia-Pichel et al., 2003b). BSC play important roles in arid ecosystem productivity and are responsible for significant nitrogen (N) flux (for review of BSC N-fixation see Belnap (2003)). For example, N-input via N-fixation versus atmospheric deposition was predominant in five times as many BSC samples from North America, Africa and Australia (Evans and Belnap, 1999). The presence of BSC is positively correlated with vascular plant survival due in part to BSC ecosystem N contributions (for review of BSC-vascular plant interactions see Belnap et al. (2003)). Climate change and disturbance alter BSC microbial community structure and membership and therefore can alter diazotroph diversity and the BSC N-budget.

BSC N-fixation rate studies (typically employing the acetylene reduction assay (ARA)) have explored BSC diazotroph activity across various ecological gradients. Reported BSC N-fixation rates vary

significantly (Evans and Lange, 2001). The reasons for this variability are complex and likely include the spatial heterogeneity of BSC (Evans and Lange, 2001) and the impact of recent environmental conditions on N-fixation rates (see Belnap (2001) for discussion). Moreover, the ARA assay is subject to methodological artifacts that preclude cross-study and possibly intra-study but inter-environment type comparisons (see Belnap (2001) for review). Nonetheless, mature BSC N-fixation rate measurements have been higher than younger, developing BSC N-fixation rate measurements (Belnap, 2002; Yeager et al., 2004). This difference may be due to the proliferation of heterocystous *Cyanobacteria* in older mats and is consistent with the theory that heterocystous *Cyanobacteria* are the primary BSC diazotrophs. Alternatively, the N-fixation rate differences between young and old BSC might be attributable to methodological artifacts. For instance, Johnson et al. (2005) show that N-fixation rates peak at a lower depth in developing BSC as compared to mature BSC. When N-fixation is measured from intact cores of developing BSC the measurement may be artifactually low due to delayed acetylene/ethylene diffusion through the crust to and from the peak N-fixation rate depth in a typical ARA incubation timeframe. Diffusion would not be an issue when measuring N-fixation rates in mature crust as nitrogenase activity peaks near the surface. When total N-fixation rates were calculated by integrating rates over 1-3 mm depth slices along full BSC cores (thus mitigating ethene/acetylene flux limitations), N-fixation rate differences between developing and mature BSC were not statistically significant (Johnson et al., 2005).

Molecular studies of BSC microbial diversity include explorations of the BSC microbial community vertical profile (Garcia-Pichel et al., 2003a), BSC *nifH* gene content surveys (e.g. Yeager et al. (2004), Yeager et al. (2012), Yeager et al. (2006) and Steppe et al. (1996)), and next-generation-sequencing (NGS) enabled studies of BSC SSU rRNA gene content across wide geographic ranges (Garcia-Pichel et al., 2013; Steven et al., 2013). *nifH* surveys have been conducted across BSC development stages (Yeager et al., 2004), as well as across seasons, temperatures and precipitation gradients (Yeager et al., 2012). Mature, more fully developed BSC possess greater numbers of heterocystous *Cyanobacteria* (e.g. *Nostoc*, *Scytonema*) than developing BSC but both young and old BSC are dominated by non-heterocystous *Cyanobacteria* (*Microcoleus vaginatus* or *M. steenstrupii*) (Yeager et al., 2004; Garcia-Pichel et al., 2013). Young or recently disturbed BSC are often described as "light" in appearance relative to "dark" mature BSC (Belnap, 2002; Yeager et al., 2004). Heterocystous *Cyanobacteria* are the numerically dominant BSC diazotrophs in *nifH* clone libraries (Yeager et al., 2006, 2004, 2012) although an early survey of Colorado Plateau BSC *nifH* diversity recovered *nifH* genes related to *Gammaproteobacteria* as well as a clade that included *nifH* genes from the anaerobes *Clostridium pssteurianum*, *Desulfovibrio gigas* and *Chromatium buideri*. Specifically, Yeager et al. (2006)—in a study of overall BSC *nifH* diversity—categorized 89% of 693 *nifH* sequences derived from Colorado Plateau and New Mexico BSC samples as heterocystous cyanobacterial (non-cyanobacterial *nifH* sequences were largely attributed to alpha- and beta- *proteobacteria*). The heterocystous cyanobacterial BSC diazotrophs fall into three genera, *Scytonema*, *Spirirestis*, and *Nostoc* (Yeager et al., 2006, 2012).

The influence of microbial community membership and structure on BSC N-fixation is an ongoing research question (Belnap, 2013). While the presence/abundance of heterocystous *Cyanobacteria* has been proposed as the mechanism behind increased N-fixation in mature BSC, it is unclear if mature BSC actually fix more N (see Johnson et al. (2005)). More studies are necessary to elucidate the microbial membership influence on BSC N-fixation and to determine if heterocystous *Cyanobacteria* are the only keystone diazotrophs. The first step in defining structure function relationships with respect to N-fixation is a full accounting of BSC diazotrophs. Towards this end we conducted  $^{15}\text{N}_2$  DNA stable isotope probing (DNA-SIP) experiments with light, developing Colorado Plateau BSC. DNA-SIP with  $^{15}\text{N}_2$  has not been attempted with BSC. DNA-SIP provides an accounting of *active* diazotrophs whereas *nifH* clone libraries account for microbes with the genomic potential for N-fixation. Further, we track the distribution of putative diazotrophs uncovered in this study through collections of NGS SSU rRNA libraries from BSC microbial diversity surveys over a range of spatial scales and soil types (Garcia-Pichel et al., 2013; Steven et al., 2013).

### 3 RESULTS

#### 3.1 ORDINATION OF CSCL GRADIENT FRACTION SSU RRNA LIBRARIES

BSC were incubated for 4 days in the presence or absence of  $^{15}\text{N}_2$  and DNA was extracted for DNA-SIP at 2 and 4 days. Fractionation of CsCl gradients permitted separation of DNA on the basis of buoyant density. Ordination of Bray-Curtis (Bray and Curtis, 1957) distances between SSU-rRNA amplicon sequence collections from gradient fractions reveals that labeled gradient fraction (i.e. gradient fractions of DNA from  $^{15}\text{N}_2$  incubations) sequence collections diverge from control (i.e. DNA from incubations without  $^{15}\text{N}_2$ ) at the “heavy“ of the CsCl gradients (Figure 1 and Figure S2). Although the density position of gradient fractions from different gradients do not match perfectly, fraction pairs from corresponding control versus labeled gradients can be constructed by pairing control gradient fractions with their closest density neighbors/fractions from corresponding labeled gradients. If a gradient fraction did not have a mate within a density difference of 0.003 g/mL it remained unpaired. Bray-Curtis distance between the fraction pairs is positively correlated to the density of the labeled fraction (p-value: 4.536e-05,  $r^2$ : 0.434) (inset Figure S2). Additionally, differences among label/control groups with heavy fractions are statistically significant by the Adonis test (p-value: 0.001,  $r^2$ : 0.18) (Anderson, 2001). The first principal axis appears to be correlated with fraction density (Figure S2) and the Adonis test p-value for density versus pairwise Bray-Curtis distances with all CsCl fraction libraries is 0.001 ( $r^2$  0.111).

#### 3.2 IDENTITIES OF OTUS RESPONSIVE TO $^{15}\text{N}_2$

A statistically significant increase in OTU abundance in heavy fractions of  $^{15}\text{N}_2$  labeled samples relative to corresponding gradient fractions from controls provides evidence for OTUs that have incorporated  $^{15}\text{N}$  into their DNA. Specifically, we compared OTU proportion means between labeled and control samples from heavy gradient fractions using statistics developed to find differentially expressed genes with RNASeq data (McMurdie and Holmes, 2014; Love et al., 2014). p-values were adjusted by the BH method (Benjamini and Hochberg, 1995) and we used a false discovery rate (FDR) cutoff of 0.10 (typical FDR threshold in gene expression data analysis, (Love et al., 2014)) to reject the null hypothesis that labeled versus control proportion mean differences were below a chosen threshold (see methods). With the above methods 38 OTUs had labeled versus control proportion mean difference adjusted p-values below 0.10 for one or both incubation days. These OTUs likely incorporated  $^{15}\text{N}$  into DNA ( $^{15}\text{N}_2$  “responders”). Of these 38, 26 are annotated as *Firmicutes*, 9 as *Proteobacteria*, 2 as *Acidobacteria* and 1 as *Actinobacteria* (Figure 3, Figure 2). If the OTUs are ranked by descending, moderated proportion mean labeled:control ratios, the top 10 ratios (i.e. the 10 OTUs that were most enriched in the labeled gradients considering only heavy fractions) are either *Firmicutes* (6 OTUs) or *Proteobacteria* (4 OTUs) (Figure 4). *Proteobacteria* OTU centroid sequences for the top 10 responders all share high identity (>98.48% identity, Table 1) with cultivars from genera known to possess diazotrophs including *Klebsiella*, *Shigella*, *Acinetobacter*, and *Ideonella*. None of the *Firmicutes* OTUs in the top 10 responders share greater than 97% sequence identity with sequences in the LTP database (release 115) (see Table 1).

If we run a second test of differential OTU abundance with the null hypothesis that OTU abundance is greater (above a threshold) in labeled, heavy gradient fractions versus control, heavy gradient fractions, we can count OTUs that likely did not respond to the label. There were 58 and 70 “non-responders” at days 2 and 4, respectively. 208 and 233 of 2,127 and 2,160 OTUs passed our sparsity threshold (OTUs had to have counts in at least 62.5% of heavy fractions) for days 2 and 4, respectively..

#### 3.3 COMPARISON OF SEQUENCE COLLECTIONS AT “STUDY”-LEVEL

**3.3.1 Comparisons of OTU content:** There were 3,079 OTUs (209,354 total sequences after quality control) in the DNA-SIP data, 3,203 OTUs (129,033 total sequences after quality control) in the Garcia-Pichel et al. (2013) study, and 2,481 OTUs (129,358 total sequences after quality control) in the Steven

et al. (2013) study. Of the 4,340 OTU centroids established for this study (including sequences from Steven et al. (2013) and Garcia-Pichel et al. (2013)) 445 have matches in the Living Tree Project (LTP) (a collection of 16S gene sequences for all sequenced type strains (Yarza et al., 2008)) at greater or equal than 97% (LTP version 115). That is, 445 of 4,340 OTUs are closely related to cultivars. The DNA-SIP data set shares 56% OTUs with the Steven et al. (2013) data and 46% of OTUs with the Garcia-Pichel et al. (2013) data (where total OTUs are from the combined data for each pairwise comparison). The Steven et al. (2013) and Garcia-Pichel et al. (2013) share 46% of OTUs.

**3.3.2 Comparisons of Taxonomic Content:** *Cyanobacteria* and *Proteobacteria* were the top two phylum-level sequence annotations for all three studies but only the DNA-SIP data had more *Proteobacteria* annotations than *Cyanobacteria*. *Proteobacteria* represented the 29.8% of sequence annotations in DNA-SIP data as opposed to 17.8% and 19.2% for the Garcia-Pichel et al. (2013) and Steven et al. (2013) data, respectively. There is a stark contrast in the total percentage of sequences annotated as *Firmicutes* between the raw environmental samples and the DNA-SIP data. *Firmicutes* represent only 0.21% and 0.23% of total phylum level sequence annotations in the Steven et al. (2013) and Garcia-Pichel et al. (2013) studies, respectively (Figure S1). In the DNA-SIP sequence collection *Firmicutes* make up 19% of phylum level sequence annotations. Also in sharp contrast for the DNA-SIP versus environmental data is the number of putative heterocystous *Cyanobacteria* sequences. Only 0.29% of *Cyanobacteria* sequences in the DNA-SIP data are annotated as belonging to "Subsection IV" which is the heterocystous order of *Cyanobacteria* in the Silva taxonomic nomenclature (Pruesse et al., 2007). In the Steven et al. (2013) and Garcia-Pichel et al. (2013) studies 15% and 23%, respectively, of *Cyanobacteria* sequences are annotated as belonging to "Subsection IV".

### 3.4 DISTRIBUTION OF BSC DIAZOTROPHS IN ENVIRONMENTAL SAMPLES

**3.4.1 Clostridiaceae:** Five of the 6 *Firmicutes* in the top 10 responder OTUs (above) belong in the *Clostridiaceae*. We only observed one of these strongly responding *Clostridiaceae* in the data presented by Garcia-Pichel et al. (2013), "OTU.108" (closest BLAST hit in LTP Release 115 – *Caloramotor proteoclasticus*, BLAST %ID 96.94, Accession X90488). OTU.108 was found in two samples both characterized as "light" crust. One other *Clostridiaceae* OTU with a proportion mean ratio (labeled:control) p-value less than 0.10 but outside the top 10 responders was found in the Garcia-Pichel et al. (2013) data (a "light" crust sample) (Figure 2). None of the strongly responding *Clostridiaceae* were found in the sequences provided by Steven et al. (2013). *Clostridiaceae* <sup>15</sup>N-responder OTU centroid 16S sequences are generally more closely related to environmental than cultivar 16S gene sequences (Table 1, Figure 5).

**3.4.2 Proteobacteria:** One of the *Proteobacteria* OTUs in the 10 most strongly responding OTUs was found in the Garcia-Pichel et al. (2013) sequences (closest BLAST hit in LTP Release 115, BLAST %ID 100, Accession ZD3440, *Acinetobacter johnsonii*). None of the strongly responding *Proteobacteria* OTUs were found in the Steven et al. (2013) sequences. There were 133 responder OTU-sample occurrences (responder OTU was found in a sample library) in the Steven et al. (2013) data. 83 were in "below crust" samples, 50 in BSC samples (see Figure 2).

**3.4.3 Other taxa:** Two <sup>15</sup>N-responsive OTUs were found in an extensive number of environmental samples (61 of 65 samples from the combined data sets of Garcia-Pichel et al. (2013) and Steven et al. (2013)). Both OTUs were annotated as *Acidobacteria* but shared little sequence identity to any cultivar SSU rRNA gene sequences in the LTP (Release 115), with best LTP BLAST hits of 81.91 and 81.32% identity. Additionally, the evidence for <sup>15</sup>N incorporation for each OTU was weak relative to other putative responders (adjusted p-values of 0.090 and 0.096). Of the remaining 36 stable isotope responder OTUs, only 14 were observed in the environmental data (Figure 2, Figure S5).



## 4 DISCUSSION

### 4.1 STUDY-LEVEL DIFFERENCES

163 SIP places focus upon organisms based on isotope incorporation and has the ability to detect activity by  
 164 low abundance members of the community. DNA from OTUs that incorporate  $^{15}\text{N}$  into their biomass  
 165 moves towards the heavy end of the CsCl gradient and therefore OTUs in “labeled” DNA are enriched  
 166 in the full data pool relative to bulk DNA. Phylum-level taxonomic annotations of  $^{15}\text{N}$ -responsive OTUs  
 167 (i.e. *Firmicutes* and *Proteobacteria*) are enriched in the DNA-SIP data relative to environmental data  
 168 (Figure S1).

### 4.2 ORDINATION OF CSCL GRADIENT FRACTION 16S RRNA GENE SEQUENCE COLLECTIONS

169 The ordination of Bray-Curtis distances between CsCl gradient fraction 16S sequence collections show  
 170 that control fractions differ from labeled fractions in the “heavy” range of the CsCl gradients (Figure S2).  
 171 If each control fraction is paired to the labeled fraction from the same incubation day for which it is closest  
 172 in density, there is a positive and statistically significant correlation between Bray-Curtis distances within  
 173 fraction pairs and density of the pair (see inset Figure S2). Therefore, the “heavy” end of the control and  
 174 labeled gradients differ and the OTUs enriched in the labeled fractions (relative to control) would have  
 175 incorporated  $^{15}\text{N}$  into their DNA during the incubation timeframe.

### 4.3 BSC DIAZOTROPHS IDENTIFIED IN THE STUDY

176 BSC N-fixation has long been attributed to heterocystous *Cyanobacteria* and molecular microbial ecology  
 177 surveys of BSC *nifH* gene content have been consistent with this hypothesis finding cyanobacterial *nifH*  
 178 types to be numerically dominant in *nifH* gene libraries (Yeager et al., 2006, 2004, 2012). Even poorly  
 179 developed BSC samples have yielded predominantly cyanobacterial *nifH* genes (Yeager et al., 2004).  
 180 And, “sub-biocrust” samples have yielded *entirely* heterocystous cyanobacterial *nifH* genes (Yeager  
 181 et al., 2012). It is possible, however, that PCR-driven molecular surveys of *nifH* gene content have  
 182 been biased against non-heterocystous *Cyanobacteria*. In general the *nifH* PCR primers used by Yeager  
 183 et al. (2006, 2004, 2012) (19F and *nifH*3) for the first round of nested PCR have broad specificity and  
 184 display at least 86% *in silico* coverage for *Proteobacteria*, *Cyanobacteria* and “Cluster III” *nifH* reference  
 185 sequences (Gaby and Buckley, 2012). In the second round of the nested PCR protocol (Yeager et al.,  
 186 2006, 2004, 2012), primer *nifH*11 is ‘slightly biased against “Cluster III” (50% coverage) but biased  
 187 in favor of *Proteobacteria* (79% *in silico* coverage against 67% for *Cyanobacteria*) and *nifH*22 matches  
 188 *Proteobacteria*, *Cyanobacteria* and “Cluster III” reference sequences poorly (16%, 23% and 21% *in silico*  
 189 coverage, respectively) (Gaby and Buckley, 2012). Unfortunately, it is difficult to assess or quantify this  
 190 bias (in either direction) without knowing the *nifH* gene content *de novo*. Another potential bias in favor of  
 191 *Cyanobacteria* in BSC *nifH* gene libraries is heterocysts (the specialized N-fixing cells along the trichome  
 192 of filamentous heterocystous *Cyanobacteria* such as *Nostoc* and *Scytonema*) may be overrepresented  
 193 with respect to non-cyanobacterial diazotrophs because heterocysts make up a fraction cells along a  
 194 trichome and even non-heterocyst cells in a trichome will possess the *nifH* gene. Polyploidy could further  
 195 exacerbate this bias, as many *Cyanobacteria* are estimated to have multiple genome copies per cell (Griese  
 196 et al., 2011). Moreover, it should also be noted that *nifH* gene content is not directly extrapolable to  
 197 the taxonomic relative abundances of nitrogenase proteins. Regardless, our results suggest that BSC N-  
 198 fixation may include a significant non-cyanobacterial component that requires further assessment across  
 199 a more comprehensive sampling of BSC types.

200 We did not observe evidence for N-fixation by heterocystous *Cyanobacteria* in the “light” crust samples  
 201 used in this study. One possible explanation for our results is that the “light”, still developing BSC samples  
 202 used in this study possessed too few heterocystous *Cyanobacteria* to statistically evaluate their  $^{15}\text{N}$ -  
 203 incorporation. Indeed, only 0.29% of sequences from this study’s DNA-SIP 16S rRNA gene sequence

libraries were from heterocystous *Cyanobacteria* (see results) as opposed to 15% and 23% of total sequences in the Steven et al. (2013) and Garcia-Pichel et al. (2013) data, respectively. Nonetheless, we would still expect even low abundance diazotrophs to show evidence for  $^{15}\text{N}$ -incorporation, provided sequence counts were not too sparse in heavy fractions. The OTUs defined by selected heterocystous *Cyanobacteria* sequences presented in Yeager et al. (2006), however, all fall below the sparsity threshold used in our analysis (see methods). Given the sparsity of heterocystous *Cyanobacteria* sequences in the DNA-SIP data set, it is not possible to assess whether heterocystous *Cyanobacteria* incorporated  $^{15}\text{N}$  during the incubation. It should be noted that "light" and in particular "sub-biocrust" samples possess much less heterocystous *Cyanobacteria* in general (Figure S3) so the samples used in this study are not necessarily unrepresentative of typical poorly developed BSC simply because they are lacking heterocystous *Cyanobacteria*.

The OTUs that did appear to incorporate  $^{15}\text{N}$  during the incubation were predominantly *Proteobacteria* and *Firmicutes*. The *Proteobacteria* OTUs for which  $^{15}\text{N}$ -incorporation signal was strongest all shared high sequence identity ( $\geq 98.48\%$  sequence identity) with 16S sequences from cultivars in genera with known diazotrophs (Table 1). The *Firmicutes* that displayed signal for  $^{15}\text{N}$ -incorporation (predominantly *Clostridiaceae*) were not closely related to any cultivars (Table 1, Figure 5). These BSC *Clostridiaceae* diazotrophs represent a gap in culture collections. As culture-based ecophysiological studies have proven useful towards explaining ecological phenomena in BSC 16S rRNA gene sequence libraries (Garcia-Pichel et al., 2013), it would seem that these putative *Clostridiaceae* diazotrophs would be prime candidates for targeted culturing efforts. Assessing the physiological response of these diazotrophic *Clostridiaceae* to temperature would be useful for predicting how climate change will affect the BSC nitrogen budget. *Gamma-proteobacteria* and spore-forming *Firmicutes* are classic opportunistic lineages that would presumably be suited to the boom/bust BSC environment. The compatible solutes produced and secreted by cyanobacteria in response to dessication and subsequent wetting could produce a local C-rich environment. Diazotrophs would be uniquely suited to respond quickly in C-rich but N-poor conditions.

Although too undersampled in the environmental data sets to reach statistical conclusions,  $^{15}\text{N}$ -responsive OTUs were found more often in below crust samples (as opposed to BSC samples) in the Steven et al. (2013) data and in "light" BSC samples in the Garcia-Pichel et al. (2013) data (Figure S5). This result generates some hypotheses that are counter to prior discussions regarding BSC diazotroph temporal dynamics (keeping in mind this phenomenon has not been evaluated statistically). Specifically, the transition of BSC from a light colored, developing crust to a dark, mature crust may not mark the emergence of diazotrophs in BSC but rather the transition of the diazotroph community from heterotroph dominance to cyanobacteria. Additionally, the soil beneath BSC may contribute significantly to the N budget in arid ecosystems.

#### 4.4 SEQUENCING DEPTH

Rarefaction curves of all samples from Steven et al. (2013) and Garcia-Pichel et al. (2013) are still sharply increasing especially for "below crust" samples (Figure S4). Parametric richness estimates of BSC diversity indicate the Steven et al. (2013) and Garcia-Pichel et al. (2013) sequencing efforts recovered on average 40.5% (sd. 9.99%) and 45.5% (sd. 11.6%) of existing 16S OTUs from samples (inset Figure S4), respectively. Further, the Steven et al. (2013) and Garcia-Pichel et al. (2013) sequence collections only share 57.6% of total OTUs found in at least one of the studies. In fact, this study shares more OTUs with Steven et al. (2013), 62.4% of OTUs in the combined data, than the Steven et al. (2013) study shares with Garcia-Pichel et al. (2013). Therefore, it is not alarming that few of the  $^{15}\text{N}$ -responsive OTUs were found by Garcia-Pichel et al. (2013) and Steven et al. (2013), it is important to point out that even next-generation sequencing efforts of BSC 16S rRNA genes have only shallowly sampled the full diversity of BSC microbes.

## 4.5 CONCLUSION

Heterocystous *Cyanobacteria* are key contributors to the BSC N-budget, but, the  $^{15}\text{N}$ -responsive OTUs found in this study and the *nifH* gene sequences from Steppe et al. (1996) in addition to the N-fixation rate data presented by (Johnson et al., 2005) suggest there may be significant non-cyanobacterial BSC diazotrophs specifically within the *Clostridiaceae* and *Proteobacteria*. It seems clear that heterocystous *Cyanobacteria* increase in abundance with BSC age (Yeager et al., 2004). It is less clear if this transition marks the emergence of diazotrophy versus a re-structuring of the BSC diazotroph community from one dominated by *Firmicutes* and *Proteobacteria* to one predominantly heterocystous *Cyanobacteria*. DNA-SIP is a valuable tool in the molecular microbial ecologist's toolbox for identifying members of microbial community functional guilds (Neufeld et al., 2007). PCR-based surveys of diagnostic marker genes and DNA-SIP are both used to connect microbial phylogenetic types to microbial activities, but they occupy a non-overlapping set of strengths and weaknesses. Combined these tools can powerfully reveal connections between ecosystem membership/structure and function. Here we supplement previous surveys of BSC *nifH* diversity, a diagnostic marker PCR-driven approach, with  $^{15}\text{N}_2$  DNA-SIP, and, while we do not confirm previous results, we expand knowledge of BSC diazotroph diversity. Predicting BSC N-fixation with respect to climate change, altered precipitation regimes and physical disturbance requires a careful accounting of diazotrophs including non-cyanobacterial types.

## 5 MATERIALS AND METHODS

### 5.1 BSC SAMPLING AND INCUBATION CONDITIONS

Light crust samples (37.5 cm<sup>2</sup>, average mass 35 g) were incubated in sealed chambers under controlled atmosphere and in the light for 4 days. Crusts were dry prior to time zero and were wetted at initiation of experiment. Treatments included control air (unenriched headspace) and enriched air (>98% atom  $^{15}\text{N}_2$ ) headspace. Samples were taken at 2 days and 4 days incubation. Acetylene reduction rates were measured daily. DNA was extracted from 1 g of crust. Samples were taken from Green Butte, Arizona as previously described (site CP3, Beraldi-Campesi et al. (2009)). All samples were from light crusts as described by Johnson et al. (2005).

### 5.2 DNA EXTRACTION

DNA from each sample was extracted using a MoBio PowerSoil DNA Isolation Kit (following manufacturers protocol, but substituting a 2 minute bead beating for the vortexing step), and then gel purified. Extracts were quantified using PicoGreen nucleic acid quantification dyes (Molecular Probes).

### 5.3 DNA-SIP

Gradient density centrifugation of DNA was undertaken in 4.7 mL polyallomer centrifuge tubes in a TLA-110 fixed angle rotor (both Beckman Coulter) in CsCl gradients with an average density of 1.725 g/mL. Average density for all prepared gradients was checked with an AR200 refractometer before runs. Between 2.5-5  $\mu\text{g}$  of DNA extract was added to the CsCl solution (15mM Tris-HCl, pH 8; 15mM EDTA; 15mM KCl), and gradients were run under conditions of 20C for 67 hours at 55,000 rpm (Buckley et al.). Centrifuged gradients were fractionated from bottom to top in 36 equal fractions of 100  $\mu\text{L}$ , using a by syringe pump as described Manefield et al. (2002). The density of each fraction was determined using an AR200 refractometer modified to accommodate 5ul samples (Buckley et al.). DNA in each fraction was desalted on a filter plate (PALL, AcroPrep Advance 96 Filter Plate, Product Number 8035), using four washes with 300 $\mu\text{L}$  TE per fraction. After each wash, the filter plate was spun at 500 g for 10 minutes, with a final spin of 20 minutes. Fractions were resuspended in 50 uL of TE buffer.

## 5.4 PCR, LIBRARY NORMALIZATION AND DNA SEQUENCING

Barcoded PCR of bacterial and archaeal 16S rRNA genes, in preparation for 454 Pyrosequencing, was carried out using primer set 515F/806R (Walters et al., 2011) (primers purchased from Integrated DNA Technologies). The primer 806R contained an 8 bp barcode sequence, a "TC" linker, and a Roche 454 B sequencing adaptor, while the primer 515F contained the Roche 454 A sequencing adapter. Each 25  $\mu$ L reaction contained 1x PCR Gold Buffer (Roche), 2.5 mM MgCl<sub>2</sub>, 200  $\mu$ M of each of the four dNTPs (Promega), 0.5 mg/mL BSA (New England Biolabs), 0.3  $\mu$ M of each primers, 1.25 U of Amplitaq Gold (Roche), and 8  $\mu$ L of template. Each sample was amplified in triplicate. Thermal cycling occurred with an initial denaturation step of 5 minutes at 95C, followed by 40 cycles of amplification (20s at 95C, 20s at 53C, 30s at 72C), and a final extension step of 5 min at 72C. Triplicate amplicons were pooled and purified using Agencourt AMPure PCR purification beads, following manufacturers protocol. Once cleaned, amplicons were quantified using PicoGreen nucleic acid quantification dyes (Molecular Probes) and pooled together in equimolar amounts. Samples were sent to the Environmental Genomics Core Facility at the University of South Carolina (now Selah Genomics) to be run on a Roche FLX 454 pyrosequencing machine.

## 5.5 DATA ANALYSIS

All code to take raw sequencing data through the presented figures can be found at:

[http://nbviewer.ipython.org/github/chuckpr/NSIP\\_data\\_analysis](http://nbviewer.ipython.org/github/chuckpr/NSIP_data_analysis)

**5.5.1 Sequence quality control** Sequences were initially screened by maximum expected errors at a specific read length threshold (Edgar, 2013) which has been shown to be as effective as denoising reads with respect to removing pyrosequencing errors. Specifically, reads were first truncated to 230 nucleotides (nt) (all reads shorter than 230 nt were discarded) and any read that exceeded a maximum expected error threshold of 1.0 was removed. After truncation and max expected error trimming, 91% of original reads remained. The first 30 nt representing the forward primer and barcode on high quality, truncated reads were trimmed. Remaining reads were taxonomically annotated using the "UClust" taxonomic annotation framework in the QIIME software package (Caporaso et al., 2010; Edgar, 2010) with cluster seeds from Silva SSU rRNA database (Pruesse et al., 2007) 97% sequence identity OTUs as reference (release 111Ref). Reads annotated as "Chloroplast", "Eukaryota", "Archaea", "Unassigned" or "mitochondria" were culled from the dataset. Finally, reads were aligned to the Silva reference alignment provided by the Mothur software package (Schloss et al., 2009) using the Mothur NAST aligner (DeSantis et al., 2006). All reads that did not appear to align to the expected amplicon region of the SSU rRNA gene were discarded. Quality control parameters removed 34,716 of 258,763 raw reads.

**5.5.2 Sequence clustering** Sequences were distributed into OTUs using the UParse methodology (Edgar, 2013). Specifically, cluster seeds were identified using USearch with a collection of non-redundant reads sorted by count as input. The sequence identity threshold for establishing a new OTU centroid was 97%. After initial cluster centroid selection, select 16S rRNA gene sequences trimmed to the same alignment positions as the other centroids from Yeager et al. (2006) were added to the centroid collection. Specifically, Yeager et al. (2006) Colorado Plateau or Moab, Utah sequences were added which included the 16S rRNA gene sequences for *Calothrix* MCC-3A (accession DQ531700.1), *Nostoc commune* MCT-1 (accession DQ531903), *Nostoc commune* MFG-1 (accession DQ531699.1), *Scytonema hyalinum* DC-A (accession DQ531701.1), *Scytonema hyalinum* FGP-7A (accession DQ531697.1), *Spirirestis rafaensis* LQ-10 (accession DQ531696.1). Centroid sequences that matched selected Yeager et al. (2006) sequences with greater than to 97% sequence identity were subsequently removed from the centroid collection. With USearch/UParse, potential chimeras are identified during OTU centroid selection and are not allowed to become cluster centroids effectively removing chimeras from the read pool. All quality controlled reads were then mapped to cluster centroids at an identity threshold of 97% again using USearch. 95.6% of



quality controlled reads could be mapped to centroids. Unmapped reads do not count towards sample counts and are essentially removed from downstream analyses. The USearch software version for cluster generation was 7.0.1090.

*5.5.3 Merging data from this study, Garcia-Pichel et al. (2013), and Steven et al. (2013)* As only sequences without corresponding quality scores were publicly available from Garcia-Pichel et al. (2013) and Steven et al. (2013), these data sets were only quality screened by determining if they covered the expected region of the 16S rRNA gene (described above). All data (this study, Garcia-Pichel et al. (2013) and Steven et al. (2013)) were included as input to USearch for OTU centroid selection and subsequent mapping to OTU centroids.

*5.5.4 Phylogenetic tree* The alignment for the "*Clostridiaceae*" phylogeny was created using SSU-Align which is based on Infernal (Nawrocki and Eddy, 2013; Nawrocki et al., 2009). Columns in the alignment that were not included in the SSU-Align covariance models or were aligned with poor confidence (less than 95% of characters in a position had posterior probability alignment scores of at least 95%) were masked for phylogenetic reconstruction. Additionally, the alignment was trimmed to coordinates such that all sequences in the alignment began and ended at the same positions. The "*Clostridiaceae*" tree included all top BLAST hits (parameters below) for  $^{15}\text{N}$  *Clostridiaceae* responders in the Living Tree Project database (Yarza et al., 2008) in addition to BLAST hits within a sequence identity threshold of 97% to  $^{15}\text{N}$  responders from the Silva SSURef.NR SSU rRNA database (Pruesse et al., 2007). Only one SSURef.NR115 hit per study per OTU ("study" was determined by "title" field) was selected for the tree. FastTree (Price et al., 2010) was used to build the tree and support values are SH-like scores reported by FastTree.

*Placement of short sequences into backbone phylogeny* Short sequences were mapped to the reference backbone using pplacer (Matsen et al., 2010) (default parameters). pplacer finds the edge placements that maximize phylogenetic likelihood. Prior to being mapped to the reference tree, short sequences were aligned to the reference alignment using Infernal (Nawrocki et al., 2009) against the same SSU-Align covariance model used to align reference sequences.

*5.5.5 BLAST searches* BLAST searches were done with the "blastn" program from BLAST+ toolkit (Camacho et al., 2009) version 2.2.29+. Default parameters were always employed and the BioPython (Cock et al., 2009) BLAST+ wrapper was used to invoke the blastn program. Pandas (McKinney, 2012) and dplyr (Wickham and Francois, 2014) were used to parse and munge BLAST output tables.

*5.5.6 Identifying OTUs that incorporated  $^{15}\text{N}$  into their DNA* SIP is a culture-independent approach towards defining identity-function connections in microbial communities (Buckley, 2011; Neufeld et al., 2007). Microbes incubated in the presence of  $^{13}\text{C}$  or  $^{15}\text{N}$  labeled substrates can incorporate the stable heavy isotope into biomass if they participate in the substrate's transformation. Stable isotope labeled nucleic acids can then be separated from unlabeled by buoyant density in a CsCl gradient. As the buoyant density of a macromolecule is dependent on many factors in addition to stable isotope incorporation (e.g. GC-content in nucleic acids (Youngblut and Buckley, 2014)), labeled nucleic acids from one microbial population may have the same buoyant density of unlabeled nucleic acids from another (i.e. each population's nucleic acids would be found at the same point along a density gradient although only one population's nucleic acids are labeled). Therefore it is imperative to compare density gradients with nucleic acids from heavy stable isotope incubations to gradients from "control" incubations where everything mimics the experimental conditions except that unlabeled substrates are used (and all DNA would be unlabeled). By contrasting "heavy" density gradient fractions in experimental density gradients (hereafter referred to as "labeled" gradients) against heavy fractions in control gradients, the identities of microbes with labeled nucleic acids can be determined

We used an RNA-Seq differential expression statistical framework (Love et al., 2014) to find OTUs enriched in heavy fractions of labeled gradients relative to corresponding density fractions in control gradients (for review of RNA-Seq differential expression statistics applied to microbiome OTU count data see McMurdie and Holmes (2014)). We use the term differential abundance (coined by McMurdie and Holmes (2014)) to denote OTUs that have different proportion means across sample classes (in this case the only sample class is labeled/control). CsCl gradient fractions were categorized as "heavy" or "light". The heavy category denotes fractions with density values above 1.725 g/mL. Since we are only interested in enriched OTUs (labeled versus control), we used a one-sided z-test for differential abundance (the null hypothesis is the labeled:control proportion mean ratio for an OTU is less than a selected threshold). P-values were corrected with the Benjamini and Hochberg method (Benjamini and Hochberg, 1995). We selected a  $\log_2$  fold change null threshold of 0.25 (or a labeled:control proportion mean ratio of 1.19). DESeq2 was used to calculate the moderated  $\log_2$  fold change of labeled:control proportion mean ratios and corresponding standard errors. Mean ratio moderation allows for reliable ratio ranking such that high variance and likely statistically insignificant mean ratios are appropriately shrunk and subsequently ranked lower than they would be as raw ratios. To summarize, OTUs with high moderated labeled:control proportion mean ratios have higher proportion means in heavy fractions of labeled gradients relative to heavy fractions of control gradients, and therefore have likely incorporated  $^{15}\text{N}$  into their DNA during the incubation.

Although DNA-SIP is a powerful technique, analysis of DNA-SIP data is not without ambiguities. One limitation is the discrete, selected boundary in the form of a adjusted p-value threshold (or false discovery rate) that marks which OTUs we consider to be enriched in the heavy fractions of labeled CsCl gradients (and thus have likely incorporated  $^{15}\text{N}$  into their DNA during the incubation). In reality the metric we use to quantify the magnitude of an OTU's response to a stable isotope is continuous, and there is only an artificial boundary between which OTUs appear to have "responded" and which OTUs have unknown response. For this reason, we have presented all the OTUs that satisfy our "response" criteria but focused on the most strongly responding OTUs. As with any hypothesis-based statistical test, care should be taken when interpreting the significance of results where p-values are near the selected threshold for rejecting the null hypothesis.

**5.5.7 Ordination** Principal coordinate ordinations depict the relationship between samples at each time point (day 2 and 4). Bray-Curtis distances were used as the sample distance metric for ordination. The Phyloseq (McMurdie and Holmes, 2014) wrapper for Vegan (Oksanen et al., 2013) (both R packages) was used to compute sample values along principal coordinate axes. GGplot2 (Wickham, 2009) was used to display sample points along the first and second principal axes. Adonis tests Anderson (2001) were done with default number of permutations (1000).

## 5.6 RICHNESS ANALYSES

Rarefaction curves were created using bioinformatics modules in the PyCogent Python package (Knight et al., 2007). Parametric richness estimates were made with CatchAll using only the best model for total OTU estimates (Bunge, 2010).

## REFERENCES

- Marti J. Anderson. A new method for non-parametric multivariate analysis of variance. *Austral Ecology*, 26(1):32–46, Feb 2001. doi: 10.1111/j.1442-9993.2001.01070.pp.x. URL <http://dx.doi.org/10.1111/j.1442-9993.2001.01070.pp.x>.
- J. Belnap. Factors Influencing Nitrogen Fixation and Nitrogen Release in Biological Soil Crusts. In *Biological Soil Crusts: Structure Function, and Management*, pages 241–261. Springer Science +

- Business Media, 2001. doi: 10.1007/978-3-642-56475-8\_19. URL [http://dx.doi.org/10.1007/978-3-642-56475-8\\_19](http://dx.doi.org/10.1007/978-3-642-56475-8_19).
- J. Belnap. Factors Influencing Nitrogen Fixation and Nitrogen Release in Biological Soil Crusts. In Jayne Belnap and Otto L. Lange, editors, *Biological Soil Crusts: Structure, Function, and Management*, volume 150 of *Ecological Studies*, pages 241–261. Springer Berlin Heidelberg, 2003. ISBN 978-3-540-43757-4. doi: 10.1007/978-3-642-56475-8\_19. URL [http://dx.doi.org/10.1007/978-3-642-56475-8\\_19](http://dx.doi.org/10.1007/978-3-642-56475-8_19).
- J. Belnap, R. Prasse, and K.T. Harper. Influence of Biological Soil Crusts on Soil Environments and Vascular Plants. In Jayne Belnap and Otto L. Lange, editors, *Biological Soil Crusts: Structure, Function, and Management*, volume 150 of *Ecological Studies*, pages 281–300. Springer Berlin Heidelberg, 2003. ISBN 978-3-540-43757-4. doi: 10.1007/978-3-642-56475-8\_21. URL [http://dx.doi.org/10.1007/978-3-642-56475-8\\_21](http://dx.doi.org/10.1007/978-3-642-56475-8_21).
- Jayne Belnap. Nitrogen fixation in biological soil crusts from southeast Utah USA. *Biology and Fertility of Soils*, 35(2):128–135, Apr 2002. doi: 10.1007/s00374-002-0452-x. URL <http://dx.doi.org/10.1007/s00374-002-0452-x>.
- Jayne Belnap. Some Like It Hot, Some Not. *Science*, 340(6140):1533–1534, 2013. doi: 10.1126/science.1240318. URL <http://www.sciencemag.org/content/340/6140/1533.short>.
- Yoav Benjamini and Yosef Hochberg. Controlling the False Discovery Rate: A Practical and Powerful Approach to Multiple Testing. *Journal of the Royal Statistical Society. Series B (Methodological)*, 57(1):289–300, 1995. ISSN 00359246. doi: 10.2307/2346101. URL <http://dx.doi.org/10.2307/2346101>.
- H. Beraldi-Campesi, H. E. Hartnett, A. Anbar, G. W. Gordon, and F. Garcia-Pichel. Effect of biological soil crusts on soil elemental concentrations: implications for biogeochemistry and as traceable biosignatures of ancient life on land. *Geobiology*, 7(3):348–359, jun 2009. doi: 10.1111/j.1472-4669.2009.00204.x. URL <http://dx.doi.org/10.1111/j.1472-4669.2009.00204.x>.
- J. Roger Bray and J. T. Curtis. An Ordination of the Upland Forest Communities of Southern Wisconsin. *Ecological Monographs*, 27(4):325, Oct 1957. doi: 10.2307/1942268. URL <http://dx.doi.org/10.2307/1942268>.
- Daniel H. Buckley. Stable Isotope Probing Techniques Using  $^{15}\text{N}$ . In *Stable Isotope Probing and Related Technologies*, pages 129–147. American Society of Microbiology, jan 2011. doi: 10.1128/9781555816896.ch7. URL <http://dx.doi.org/10.1128/9781555816896.ch7>.
- DH Buckley, V Huangyutitham, SF Hsu, and TA Nelson. Stable isotope probing with  $^{15}\text{N}_2$  reveals novel noncultivated diazotrophs in soil. *Appl Environ Microbiol*, 73:3196–204.
- John Bunge. Estimating the Number of Species with Catchall. In *Biocomputing 2011*, pages 121–130. WORLD SCIENTIFIC, nov 2010. doi: 10.1142/9789814335058\_0014. URL [http://dx.doi.org/10.1142/9789814335058\\_0014](http://dx.doi.org/10.1142/9789814335058_0014).
- C Camacho, G Coulouris, V Avagyan, N Ma, J Papadopoulos, K Bealer, and TL Madden. BLAST+: architecture and applications. 10:421, Dec 2009.
- JG Caporaso, J Kuczynski, J Stombaugh, K Bittinger, FD Bushman, EK Costello, N Fierer, AG Pea, JK Goodrich, JI Gordon, GA Huttley, ST Kelley, D Knights, JE Koenig, RE Ley, CA Lozupone, D McDonald, BD Muegge, M Pirrung, J Reeder, JR Sevinsky, PJ Turnbaugh, WA Walters, J Widmann, T Yatsunenko, J Zaneveld, and R Knight. QIIME allows analysis of high-throughput community sequencing data. 7:335–6, 2010.
- PJ Cock, T Antao, JT Chang, BA Chapman, CJ Cox, A Dalke, I Friedberg, T Hamelryck, F Kauff, B Wilczynski, and Hoon MJ de. Biopython: freely available Python tools for computational molecular biology and bioinformatics. 25:1422–3, 2009.
- TZ Jr DeSantis, P Hugenholtz, K Keller, EL Brodie, N Larsen, YM Piceno, R Phan, and GL Andersen. NAST: a multiple sequence alignment server for comparative analysis of 16S rRNA genes. 34:W394–9, 2006.
- RC Edgar. Search and clustering orders of magnitude faster than BLAST. 26:2460–1, 2010.
- RC Edgar. UPARSE: highly accurate OTU sequences from microbial amplicon reads. 10:996–8, 2013.
- R. D. Evans and J. Belnap. Long-Term Consequences of Disturbance on Nitrogen Dynamics in an Arid Ecosystem. *Ecology*, 80(1):150–160, Jan 1999. doi: 10.1890/0012-9658(1999)080[0150:ltcodo]2.

- 0.co;2. URL [http://dx.doi.org/10.1890/0012-9658\(1999\)080\[0150:LTCODO\]2.0.CO;2](http://dx.doi.org/10.1890/0012-9658(1999)080[0150:LTCODO]2.0.CO;2).
- R. D. Evans and O. L. Lange. Biological Soil Crusts and Ecosystem Nitrogen and Carbon Dynamics. In *Biological Soil Crusts: Structure Function, and Management*, pages 263–279. Springer Science + Business Media, 2001. doi: 10.1007/978-3-642-56475-8\_20. URL [http://dx.doi.org/10.1007/978-3-642-56475-8\\_20](http://dx.doi.org/10.1007/978-3-642-56475-8_20).
- John Christian Gaby and Daniel H. Buckley. A Comprehensive Evaluation of {PCR} Primers to Amplify the {nifH} Gene of Nitrogenase. {PLOS} {ONE}, 7(7):e42149, jul 2012. doi: 10.1371/journal.pone.0042149. URL <http://dx.doi.org/10.1371/journal.pone.0042149>.
- F. Garcia-Pichel, S. L. Johnson, D. Youngkin, and J. Belnap. Small-Scale Vertical Distribution of Bacterial Biomass and Diversity in Biological Soil Crusts from Arid Lands in the Colorado Plateau. *Microbial Ecology*, 46(3):312–321, Nov 2003a. doi: 10.1007/s00248-003-1004-0. URL <http://dx.doi.org/10.1007/s00248-003-1004-0>.
- F. Garcia-Pichel, V. Loza, Y. Marusenko, P. Mateo, and R. M. Potrafka. Temperature Drives the Continental-Scale Distribution of Key Microbes in Topsoil Communities. *Science*, 340(6140):1574–1577, Jun 2013. doi: 10.1126/science.1236404. URL <http://dx.doi.org/10.1126/science.1236404>.
- Ferran Garcia-Pichel, Jayne Belnap, Susanne Neuer, and Ferdinand Schanz. Estimates of global cyanobacterial biomass and its distribution. *Algological Studies*, 109(1):213–227, 2003b.
- Marco Griese, Christian Lange, and Jrg Soppa. Ploidy in cyanobacteria. *FEMS Microbiology Letters*, 323(2):124–131, sep 2011. doi: 10.1111/j.1574-6968.2011.02368.x. URL <http://dx.doi.org/10.1111/j.1574-6968.2011.02368.x>.
- SL Johnson, CR Budinoff, J Belnap, and F Garcia-Pichel. Relevance of ammonium oxidation within biological soil crust communities. 7:1–12, 2005.
- A. Karnieli, R.F. Kokaly, N.E. West, and R.N. Clark. Remote Sensing of Biological Soil Crusts. In Jayne Belnap and Otto L. Lange, editors, *Biological Soil Crusts: Structure, Function, and Management*, volume 150 of *Ecological Studies*, pages 431–455. Springer Berlin Heidelberg, 2003. ISBN 978-3-540-43757-4. doi: 10.1007/978-3-642-56475-8\_31. URL [http://dx.doi.org/10.1007/978-3-642-56475-8\\_31](http://dx.doi.org/10.1007/978-3-642-56475-8_31).
- Rob Knight, Peter Maxwell, Amanda Birmingham, Jason Carnes, J Gregory Caporaso, Brett C Easton, Michael Eaton, Micah Hamady, Helen Lindsay, Zongzhi Liu, Catherine Lozupone, Daniel McDonald, Michael Robeson, Raymond Sammut, Sandra Smit, Matthew J Wakefield, Jeremy Widmann, Shandy Wikman, Stephanie Wilson, Hua Ying, and Gavin A Huttley. {PyCogent}: a toolkit for making sense from sequence. *Genome Biol*, 8(8):R171, 2007. doi: 10.1186/gb-2007-8-8-r171. URL <http://dx.doi.org/10.1186/gb-2007-8-8-r171>.
- M. I. Love, W. Huber, and S. Anders. Moderated estimation of fold change and dispersion for {RNA}-Seq data with {DESeq}2. Technical report, feb 2014. URL <http://dx.doi.org/10.1101/002832>.
- Frederick A Matsen, Robin B Kodner, and E Virginia Armbrust. pplacer: linear time maximum-likelihood and Bayesian phylogenetic placement of sequences onto a fixed reference tree. *BMC Bioinformatics*, 11(1):538, 2010. doi: 10.1186/1471-2105-11-538. URL <http://dx.doi.org/10.1186/1471-2105-11-538>.
- Wes McKinney. pandas: Python Data Analysis Library. Online, 2012. URL <http://pandas.pydata.org/>.
- PJ McMurdie and S Holmes. Waste not, want not: why rarefying microbiome data is inadmissible. 10:e1003531, 2014.
- EP Nawrocki and SR Eddy. Infernal 1.1: 100-fold faster RNA homology searches. 29:2933–5, Nov 2013.
- EP Nawrocki, DL Kolbe, and SR Eddy. Infernal 1.0: inference of RNA alignments. 25:1335–7, May 2009.
- JD Neufeld, J Vohra, MG Dumont, T Lueders, M Manefield, MW Friedrich, and JC Murrell. DNA stable-isotope probing. 2:860–6, 2007.
- Jari Oksanen, F. Guillaume Blanchet, Roeland Kindt, Pierre Legendre, Peter R. Minchin, R. B. O’Hara, Gavin L. Simpson, Peter Solymos, M. Henry H. Stevens, and Helene Wagner. *vegan: Community*



- Ecology Package, 2013. URL <http://CRAN.R-project.org/package=vegan>. R package version 2.0-10.
- MN Price, PS Dehal, and AP Arkin. FastTree 2—approximately maximum-likelihood trees for large alignments. 5:e9490, Mar 2010.
- E Pruesse, C Quast, K Knittel, BM Fuchs, W Ludwig, J Peplies, and FO Glckner. SILVA: a comprehensive online resource for quality checked and aligned ribosomal RNA sequence data compatible with ARB. 35:7188–96, 2007.
- PD Schloss, SL Westcott, T Ryabin, JR Hall, M Hartmann, EB Hollister, RA Lesniewski, BB Oakley, DH Parks, CJ Robinson, JW Sahl, B Stres, GG Thallinger, Horn DJ Van, and CF Weber. Introducing mothur: open-source, platform-independent, community-supported software for describing and comparing microbial communities. 75:7537–41, 2009.
- T.F. Steppe, J.B. Olson, H.W. Paerl, R.W. Litaker, and J. Belnap. Consortial N<sub>2</sub> fixation: a strategy for meeting nitrogen requirements of marine and terrestrial cyanobacterial mats. *FEMS Microbiology Ecology*, 21(3):149–156, Nov 1996. doi: 10.1111/j.1574-6941.1996.tb00342.x. URL <http://dx.doi.org/10.1111/j.1574-6941.1996.tb00342.x>.
- Blaire Steven, La Verne Gallegos-Graves, Jayne Belnap, and Cheryl R. Kuske. Dryland soil microbial communities display spatial biogeographic patterns associated with soil depth and soil parent material. *FEMS Microbiol Ecol*, 86(1):101–113, May 2013. doi: 10.1111/1574-6941.12143. URL <http://dx.doi.org/10.1111/1574-6941.12143>.
- WA Walters, JG Caporaso, CL Lauber, D Berg-Lyons, N Fierer, and R Knight. PrimerProspector: de novo design and taxonomic analysis of barcoded polymerase chain reaction primers. 27:1159–61, Apr 2011.
- Hadley Wickham. *ggplot2: elegant graphics for data analysis*. Springer New York, 2009. ISBN 978-0-387-98140-6. URL <http://had.co.nz/ggplot2/book>.
- Hadley Wickham and Romain Francois. *dplyr: dplyr: a grammar of data manipulation*, 2014. URL <http://CRAN.R-project.org/package=dplyr>. R package version 0.2.
- Pablo Yarza, Michael Richter, Jörg Peplies, Jean Euzéby, Rudolf Amann, Karl-Heinz Schleifer, Wolfgang Ludwig, Frank Oliver Glöckner, and Ramon Rosselló-Móra. The All-Species Living Tree project: A 16S rRNA-based phylogenetic tree of all sequenced type strains. *Systematic and Applied Microbiology*, 31(4):241–250, Sep 2008. doi: 10.1016/j.syapm.2008.07.001. URL <http://dx.doi.org/10.1016/j.syapm.2008.07.001>.
- Chris M. Yeager, Jennifer L. Kornosky, Rachael E. Morgan, Elizabeth C. Cain, Ferran Garcia-Pichel, David C. Housman, Jayne Belnap, and Cheryl R. Kuske. Three distinct clades of cultured heterocystous cyanobacteria constitute the dominant N<sub>2</sub>-fixing members of biological soil crusts of the Colorado Plateau USA. *FEMS Microbiology Ecology*, 60(1):85–97, 2006. doi: 10.1111/j.1574-6941.2006.00265.x. URL <http://dx.doi.org/10.1111/j.1574-6941.2006.00265.x>.
- Chris M. Yeager, Cheryl R. Kuske, Travis D. Carney, Shannon L. Johnson, Lawrence O. Ticknor, and Jayne Belnap. Response of Biological Soil Crust Diazotrophs to Season Altered Summer Precipitation, and Year-Round Increased Temperature in an Arid Grassland of the Colorado Plateau, USA. *Front. Microbio.*, 3, 2012. doi: 10.3389/fmicb.2012.00358. URL <http://dx.doi.org/10.3389/fmicb.2012.00358>.
- CM Yeager, JL Kornosky, DC Housman, EE Grote, J Belnap, and CR Kuske. Diazotrophic community structure and function in two successional stages of biological soil crusts from the Colorado Plateau and Chihuahuan Desert. 70:973–83, 2004.
- ND Youngblut and DH Buckley. Intra-genomic variation in G+C content and its implications for DNA stable isotope probing (DNA-SIP). Aug 2014.

## 6 FIGURES AND LONG TABLES

**Table 1.**  $^{15}\text{N}$  responders BLAST against Living Tree Project

OTU ID	Species Name	BLAST percent identity	accession
OTU.108	<i>Caloramator proteoclasticus</i>	96.94	X90488
OTU.14	<i>Pantoea rwandensis</i>	99.49	JF295055
	<i>Pantoea rodasii</i>	99.49	JF295053
	<i>Kluyvera intermedia</i>	99.49	AF310217
	<i>Kluyvera cryocrescens</i>	99.49	AF310218
	<i>Klebsiella variicola</i>	99.49	AJ783916
	<i>Klebsiella pneumoniae subsp. rhinoscleromatis</i>	99.49	Y17657
	<i>Klebsiella pneumoniae subsp. pneumoniae</i>	99.49	X87276
	<i>Erwinia aphidicola</i>	99.49	FN547376
	<i>Enterobacter soli</i>	99.49	GU814270
	<i>Enterobacter ludwigii</i>	99.49	AJ853891
	<i>Enterobacter kobei</i>	99.49	AJ508301
	<i>Enterobacter hormaechei</i>	99.49	AJ508302
	<i>Enterobacter cloacae subsp. dissolvens</i>	99.49	Z96079
	<i>Enterobacter cancerogenus</i>	99.49	Z96078
	<i>Enterobacter asburiae</i>	99.49	AB004744
	<i>Enterobacter amnigenus</i>	99.49	AB004749
	<i>Enterobacter aerogenes</i>	99.49	AB004750
	<i>Buttiauxella warmboldiae</i>	99.49	AJ233406
	<i>Buttiauxella noackiae</i>	99.49	AJ233405
	<i>Buttiauxella izardii</i>	99.49	AJ233404
	<i>Buttiauxella agrestis</i>	99.49	AJ233400
OTU.1673	<i>Clostridium drakei</i>	95.9	Y18813
	<i>Clostridium carboxidivorans</i>	95.9	FR733710
OTU.327	<i>Clostridium hydrogeniformans</i>	94.92	DQ196623
	<i>Clostridium amylolyticum</i>	94.92	EU037903
OTU.330	<i>Clostridium lundense</i>	96.94	AY858804
OTU.342	<i>Acinetobacter johnsonii</i>	100.0	Z93440
OTU.4037	<i>Fonticella tunisiensis</i>	93.85	HE604099
OTU.54	<i>Shigella sonnei</i>	100.0	FR870445
	<i>Shigella flexneri</i>	100.0	X96963
	<i>Escherichia fergusonii</i>	100.0	AF530475
	<i>Escherichia coli</i>	100.0	X80725
OTU.57	<i>Fonticella tunisiensis</i>	93.88	HE604099
	<i>Caloramator proteoclasticus</i>	93.88	X90488
OTU.586	<i>Vitreoscilla filiformis</i>	98.48	HM037993
	<i>Ottowia pentelensis</i>	98.48	EU518930
	<i>Ideonella dechloratans</i>	98.48	X72724
	<i>Diaphorobacter nitroreducens</i>	98.48	AB064317
	<i>Comamonas terrigena</i>	98.48	AF078772

**Figure 1.** Ordination of heavy gradient fraction sequence collections by Bray-Curtis distances.

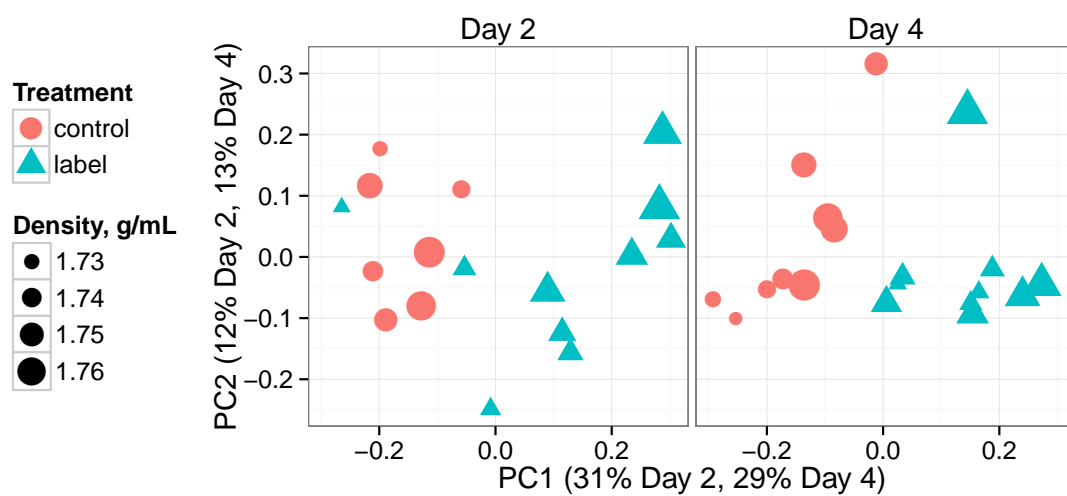


**Figure 2.** Phylogenetic trees of OTUs passing sparsity threshold for selected phyla. *A*) Point denotes OTU is classified as a  $^{15}\text{N}$  “responder”. *B*) Heatmap of moderated  $\log_2$  proportion mean ratios (labeled:control gradients) for each OTU at each incubation day. High values indicate  $^{15}\text{N}$  incorporation. *C*) Presence/absence of OTUs (black indicates presence) in lichen, light, or dark environmental samples (Garcia-Pichel et al., 2013). *D*) Presence/absence of OTUs (black indicates presence) in crust and below crust samples (Steven et al., 2013).

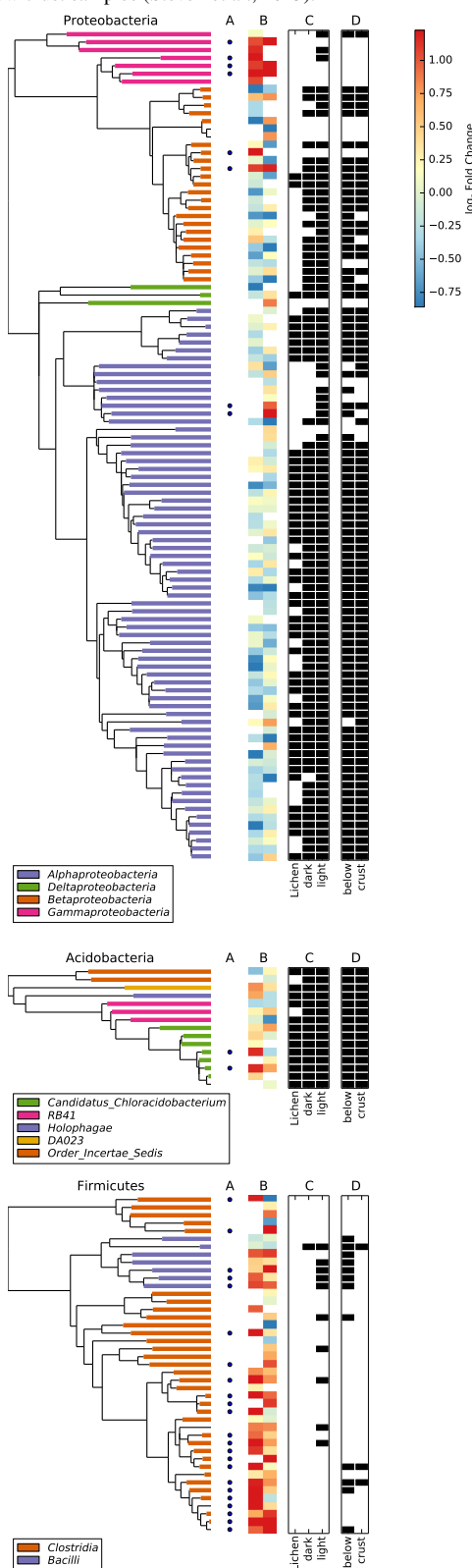




**Figure 3.** Moderated  $\log_2$  of proportion mean ratios for labeled versus control gradients (heavy fractions only, densities  $\geq 1.725$  g/mL). All OTUs found in at least 62.5% of heavy fractions at a specific incubation day are shown. Red color denotes a proportion mean ratio that has a corresponding adjusted p-value below a false discovery rate of 10% (the null model is that the proportion mean is ratio is below 0.25). The horizontal line is the proportion mean threshold for the null model, 0.25. The inset figure summarizes the taxonomy of OTUs that with proportion mean ratio p-values under 0.10 for at least one time point.



**Figure 4.** Relative abundance values in heavy fractions (density greater or equal to 1.725 g/mL) for the top 10  $^{15}\text{N}$  "responders" (putative diazotrophs, see results for selection criteria of top 10) at each incubation day. See Table 1 for BLAST results of top 10 responders against the LTP database (release 115). Point area is proportional to CsCl gradient fraction density, and color signifies control (red) or labeled (blue) treatment.



Phylogenetic tree showing relationships between various bacterial strains, primarily *Clostridium* species. Bootstrap values are indicated at the nodes. The tree is rooted at the top left. The species names are listed on the right side of the tree. The tree is color-coded: red for *Clostridium* species, blue for other species, and black for the outgroup.

Species names (from top to bottom):

- AB487053
- JX223241
- Caloramator proteoclasticus X90488
- Fonticella tunisiensis HE604099
- GU214137
- AB486915
- JX222954
- HM745428
- Clostridium algidicarnis AF127023
- Clostridium amylolyticum EU037903
- Clostridium hydrogeniformans DQ196623
- Clostridium paraputrificum X75907
- Clostridium perfringens CP000246
- Eubacterium tarantellae FR733677
- DQ129399
- GU214161
- EU250947
- FN667108
- FJ484658
- FJ382239
- DQ129397
- EF205504
- AB488371
- AB486282
- AJ226186
- AJ229218
- AB487078
- AB487139
- EU134673
- JF189151
- DQ129245
- HQ397206
- AM697455
- FJ889263
- JF698001
- Y15985
- GQ264258
- HE589855
- EF632748
- RJ892892
- JN379402
- HM269045
- AB479046
- JF681410
- JX223165
- AJ617870
- AY548785
- KC001367
- AJ229224
- AB486118
- JF815499
- AB486650
- GQ487902
- AB487171
- JF198389
- JQ815738
- AB696043
- AB487446
- AB486424
- AJ229230
- AB486908
- Clostridium carboxidivorans FR733710
- Clostridium drakei Y18813
- Clostridium aciditolerans DQ114945
- JX505285
- Clostridium nitrophenolicum AM261414
- IN899155
- KC215464
- Illyobacter delafieldii FR733681
- JX223060
- JX223421
- Clostridium lundense AY858804
- AB699886
- KC331197
- Clostridium subterminale AF241844
- Clostridium sulfidigenes EF199998
- Clostridium thiosulfatireducens AY024332
- AB600546
- HQ395208
- JF681392
- AY187622
- HM800737
- AMQH01000037
- DQ479415
- AM086139
- JQ711701
- HQ327271
- FJ946570
- FJ665184
- JF775630
- FN436154
- HE575393
- DQ248294
- FJ167457
- EF019973
- FJ592916
- JF832340
- JN540099
- GQ397026
- JX948684
- Clostridium tagluense DQ296031
- JX505301
- AB630536
- Clostridium bowmanii AJ506119
- Clostridium algariphilum AY117755
- EF589987
- HQ462514
- AJ506117
- Clostridium estertheticum subsp. laramiense AJ506115
- Clostridium estertheticum subsp. estertheticum S46734
- JX68181

## 7 SUPPLEMENTAL FIGURES



**Figure S1.** Distribution of sequences into top 9 phyla (phyla ranked by sum of all sequence annotations).



**Figure S2.** Ordination of Bray-Curtis sample pairwise distances for each incubation time. Point area is proportional to the density of the CsCl gradient fraction for each sequence library, and color/shape reflects control (red triangles) or labeled (blue circles) treatment. Inset shows Bray-Curtis distances for paired control versus labeled CsCl gradient fractions (i.e. fractions from the same incubation day and same density) against the density of the pair (p-value:  $4.526 \times 10^{-5}$ ,  $r^2$ : 0.434).



**Figure S3.** Relative abundance of selected heterocystous cyanobacterial OTUs with centroids from sequences described in Yeager et al. (2006) (see methods for selection criteria) in Steven et al. (2013) data set.



**Figure S4.** Rarefaction curves for all samples presented by Garcia-Pichel et al. (2013) and Steven et al. (2013). Inset is boxplot of estimated sampling effort for all samples in Garcia-Pichel et al. (2013) and Steven et al. (2013) (number of observed OTUs divided by number of CatchAll Bunge (2010) estimated total OTUs)





**Figure S5.** Counts of "responder" OTU occurrences in samples from Steven et al. (2013) and Garcia-Pichel et al. (2013). Steven et al. (2013) collected BSC samples (25 samples total) and samples from soil beneath BSC (17 samples total, "below" column in figure). Garcia-Pichel et al. (2013) collected samples from "dark" (9 samples total) and "light" (12 samples total) crusts in addition to "lichen" (2 samples total) dominated crusts.

